Bohlen, J.; Dobron, P.; Swiostek, J.; Letzig, D.; Chmelik, F.;
Lukac, P.; Kainer, K.U.:

On the influence of the grain size and solute content on the AE response of magnesium alloys tested in tension and compression

In: Materials Science and Engineering A (2006) Elsevier

DOI: 10.1016/j.msea.2006.02.470

On the influence of the grain size and solute content on the AE response of magnesium alloys tested in tension and compression

Jan Bohlen[1*], Patrik Dobroň[2], Jacek Swiostek[1], Dietmar Letzig[1], František Chmelík[2], Pavel Lukáč[2], Karl Ulrich Kainer[1]

[1]GKSS-Forschungszentrum GmbH, Max-Planck-Str. 1, D-21502 Geesthacht, Germany

[2]Department of Metal Physics, Charles University, Ke Karlovu 5, CZ 121 16 Prague 2, Czech Republic

*corresponding author email: jan.bohlen@gkss.de

Abstract

Tensile and compression tests were conducted for AZ31, AZ61 and AZ80 alloys. The distinctive tension/compression asymmetry in the yield behaviour was analysed for textured samples from extruded bars with various grain sizes. Parallel measurements of the acoustic emission were carried out to gather information about the relative activity of twinning and dislocation glide during deformation. The acoustic emission data are used to elaborate on the possible roles of grain size and aluminium content on the deformation behaviour.

Keywords: Magnesium alloys, AZ31, AZ61, AZ80, twinning, grain size, acoustic emission, solid solution softening

Introduction

The yield behaviour of magnesium and its alloys is well known to occur with a distinctive asymmetry, which is related to the prevalence of {10-12} twinning [1, 2]. It leads to an 86° re-orientation of grains and can contribute to the macroscopic strain when a stress component is applied in tension parallel to the c-axis or in compression perpendicular to the c-axis [3]. Therefore, in textured extruded bars, that have the basal planes preferentially oriented parallel to the extrusion direction, this asymmetry is manifested as lower yield strength in compression than in tension [4, 5, 6, 7]. This can be understood by {10-12} twinning not being favoured in tension whereas it is preferred in compression along the extrusion axis [6, 7]. The asymmetry (defined as the difference between tensile and compressive yield strength $\Delta\sigma = \sigma_{02\,tension} - \sigma_{02\,compression}$) and its relation to twinning is of importance for engineering magnesium alloys because it is the objective to decrease this difference as far as possible. It also offers the possibility to study this effect by comparing tensile and compression tests. By doing this, it is our intention to analyse the influence of grain size and the content of aluminium in AZ alloys on twinning.

Generally, the grain size dependence of the activation of deformation mechanisms in polycrystals is described according to the Hall – Petch law [8]. It describes the dependence of the yield strength σ on the average grain size d as $\sigma = \sigma_0 + k \cdot d^{-1/2}$ where σ_0 is a friction stress for dislocation movement. The slope k, called as the “Hall-Petch strength coefficient”, depends on the orientation relation between the interacting grains as well as the critical shear stresses of the activated deformation modes in both grains. It is only briefly studied, however, how far this relation describes also deformation twinning in magnesium [9]. For b.c.c. metals such a description has been shown in literature (e.g. [10]).

By using textured bars in this study, the contribution of twinning can be maximised in compression whereas it can be minimized in tension. Thus, any effect of the grain size or the content of alloying elements on twinning will be magnified and can be studied by a Hall-Petch analysis, using the tension/compression yield asymmetry. The tension and compression tests are accompanied by measurement of the acoustic emission (AE). AE is the result of transient elastic waves that occur due to a sudden release of energy from local dynamical changes in the material structure such as dislocation glide and twinning [11]. We will use this method to gain some insight into the deformation micromechanisms operating in textured bars of AZ alloys.

Experimental

Direct chill (DC)-cast billets of high-purity alloys AZ31, AZ61 and AZ80 were used in an as-cast and homogenized condition [12]. Indirect and hydrostatic extrusion trials with a number of varied parameter settings (temperature, extrusion ratio) [12, 13] were carried out to produce bars. A detailed description of the process set-ups is given in references [14, 15]. Hydrostatic extrusion was accompanied by water-cooling of the exiting profile. This method results in a finer grain size than indirectly extruded bars due to a lower adiabatic heating during extrusion [16] and the water-cooling which prevents grain growth after extrusion [4].

A universal testing machine was used for tensile and compression testing at room temperature at a constant strain rate of 10^{-3} s^{-1}. The yield strength was measured as 0,2% proof stress $\sigma_{0,2}$. In case of a number of compression tests with a pronounced elastic limit it is represented as the lower compressive yield strength σ_{lcys}. Picric acid was used [17] to reveal the grains in prepolished sections. The average grain size was determined from several micrographs using a computer-aided linear intercept measurement. The computer controlled DAKEL-XEDO-3 AE system was used to perform monitoring of AE events (two-threshold-level detection [18]). This yields a comprehensive set of AE parameters including count rates $\dot{N}_{C1}$ and $\dot{N}_{C2}$. These are count numbers per second giving the total AE counts as $\dot{N}_{C1}$ at the lower threshold level and the burst type AE counts as $\dot{N}_{C2}$ at the upper threshold level. Details can be found elsewhere [19, 20].

Results

Fig. 1 a – c shows the yield strength as a function of the grain size for AZ31, AZ61 and AZ80, respectively. It can be seen that for all three alloys the yield strength increases with decreasing grain size according to the Hall-Petch relationship for both tension and compression. Furthermore, the Hall-Petch slope is more pronounced for compression than for tension, with the result that the tension/compression asymmetry decreases with the grain size. The k values also increase for both tension and compression with increasing content of aluminium. Such clear trends were not observed for σ_0, but the σ_0 values are lower in compression than in tension.

The effect of grain size and aluminium content on the tension/compression asymmetry can be better appreciated in Fig. 2. While the asymmetry in tensile and compressive yield strength has already been clearly attributed to a different contribution of twinning to the macroscopic strain, it can be seen that the difference between tensile and compressive yield strength generally decreases with decreasing grain size. Furthermore, it also decreases with increasing content of aluminium in the alloy referring to the same grain size.

Figs. 3 and 4 show typical tension and compression stress-strain curves correlated to AE count rates at both threshold values N_{c1} and N_{c2} during testing as a function of testing time. Both, strain and testing time correspond to each other due to the constant strain rate of 10^{-3}/s. The curves were obtained from coarser-grained material with an average grain size of 12 – 16 µm. In all cases the count rates increase to a peak maximum at the beginning of plastic deformation. The peak is followed by a decrease which is different when comparing tension and compression. During tensile testing, a rather slow decrease is found with an AE activity persisting until the fracture of the samples. During compression testing, however, a somewhat "broader" maximum peak is found, which is then followed by a more rapid decrease in the AE activity especially for $\dot{N}_{C2}$ that represents signals of burst character and large amplitudes (higher threshold level). For AZ61 and AZ80 an additional increase especially of $\dot{N}_{C1}$ is found at strains between 5 – 10 % whereas for AZ31 there is a continuous decrease of the count rate. Generally, for all measurements, it shall be noted that the count rates decrease with increasing content of aluminium.

Regarding the influence of grain size on the AE count rates it has been shown elsewhere [20] that the AE count rates increase with grain size.

Discussion

In the AE measurements shown in Fig. 3 and 4, generally, the peak of the count rates near the yield point can be attributed to massive dislocation movement as well as twinning. Generally, it cannot be distinguished explicitly between these two mechanisms in the AE measurement, but it is possible to speculate based on the nature of the AE signals. A distinctive number of burst type signals occur during tensile testing that – with decreasing count rate – are visible up to the sample fracture, cannot be attributed to dislocation motion any more because this will lose its massive character when strain hardening occurs. Thus, especially the burst type signals in the latter part of the measurements may be attributed to twinning. Compared to tension, during compression testing the AE peak count rate at one point consists mainly of burst type signals that then decrease rapidly with strain. While the burst type peak is consistent with our understanding of twinning playing a preferred role during compression testing it apparently does not occur at high strains. This compares well to the *in-situ* texture measurements of Davies et al. [21] in case of a flat bar, showing a massive near 90° re-orientation of grains (that is attributed to twinning) during compression testing. This is very significant up to a strain of 3% and is almost finished at a strain of 6%.

The tension/compression asymmetry decreases with decreasing grain size. Corresponding to this, the AE count rates decrease. We attribute this to the fact that massive dislocation slip as well as twinning does occur with lower activity. It should be noted that for all bars a high elongation to fracture of 15 – 20% in tension and 10 – 15% in compression was observed, which indicates that the deformation obeys the v. Mises criterion (necessity to have at least 5 independent slip modes [22]). We cannot state which mechanisms are active, but it can be assumed that non-basal slip in general has to be active. Grain boundary sliding for finer-grained samples could also be considered. Both mechanisms will not contribute to the tensile/compression asymmetry and also not produce any additional AE.

The data obtained for the Hall-Petch strength coefficient have to be seen in the light of the pre-existing texture, which affects the Taylor orientation factor. Hence the *k*-values apply only to the particular texture and not to a random polycrystal. [23]. Thus, we only discuss the overall trends in the behaviour rather than update quantitative values. However, the *k*-value from compression tests of AZ31 compares well to the results of Barnett et al. [9]. The Hall-Petch slope in general is always higher in compression than in tension and it increases in both cases with increasing content of aluminium. The first effect indicates the strong dependence of the contribution of twinning in compression on the grain size. The latter effect has also been reported by Ono et al. [24] who explain it by solution strengthening due to aluminium. Post – stress relaxation effects [25] also indicate that solid solution strengthening due to aluminium is important for the deformation behaviour of AZ alloys. Kleiner & Uggowitzer [7] relate this directly to basal slip, but further they discuss a solution softening of prismatic slip. In summary, this means a change in the relation between the critical resolved shear stresses of basal and non-basal slip. This is likely to affect the activity of twinning which is corroborated by the fact that the tensile/compression asymmetry is lowered with increasing content of aluminium. Furthermore, a reduced twinning activity could also be a direct effect of aluminium on the twin nucleation and/or twin growth. And it should also be noted that precipitates of $Mg_{17}Al_{12}$ in AZ61 and especially in AZ80 occur at the grain boundaries as well as in the grains (see our earlier paper [20]). These will also affect twin nucleation and twin growth [26].

We also find that the count number detected throughout the measurements decreases with increasing content of aluminium (tension: 1.9×10^6 for AZ31 to 0.9×10^6 for AZ80, compression: 4×10^6 for AZ31 to 2.8×10^6 for AZ80). This is also consistent with a solution strengthening for basal slip where massive dislocation movements are somewhat suppressed and therefore do not contribute to the AE count rates any more. Furthermore, it would also be consistent with a lower twin activity reflecting the lower tensile/compression asymmetry.

Conclusions

The tensile/compression asymmetry has been shown using textured bars of alloys AZ31, AZ61 and AZ80. It is described as a geometrical effect of twinning that can better contribute to the macroscopic strain in compression rather than in tension. Acoustic emission count rates occur with massive burst type emissions at low strains during compression and corroborate the prevalence of twinning.

Aluminium as an alloying element leads to a decrease in the tension/compression asymmetry. This also corresponds to a decrease in the acoustic emission count rates. This is discussed as a decrease in the activity of twinning due to a change in the activity of basal and non-basal slip. Furthermore the influence of solute aluminium on the twinning activity has to be addressed as well as the influence of precipitates on the activity of twinning.

Acknowledgements

We appreciate technical support by Dr. Hans-Ulrich Menzel during hydrostatic extrusion trials. Also support by Dipl. Ing. Sören Müller during indirect extrusion trials as part of the “Virtual Institute – Key materials for light weight contruction” is appreciated. Financial support by the Hermann von Helmholtz Association (HGF) is acknowledged. The work also received support by the Czech Grant Agency under grant 205/03/0071.

References

[1] E. W. Kelley, W. F. Hosford Jr., Trans. TMS-AIME 242 (1968) 5.

[2] S.R. Agnew, M.H. Yoo, C.N. Tome, Acta Mater. 49 (2001) 4277.

[3] P. G. Partridge, Metall. Rev. 118 (1967) 169.

[4] J. Bohlen, S.B. Yi, J. Swiostek, D. Letzig, H. G. Brokmeier, K. U. Kainer, Scripta Mat. 53 (2005) 259.

[5] I. L. Dillamore, W.T. Roberts, Metall. Rev. 10 (1965) 271.

[6] E. A. Ball, P. B. Prangnell, Scripta Metall. 31 (1994) 111.

[7] S. Kleiner, P. J. Uggowitzer, Mat. Sci. Eng. A 379 (2004) 258.

[8] Peter Haasen: Physical Metallurgy, 3rd enl. and rev. ed., Cambridge University Press, Cambridge, 1996 (textbook).

[9] M.R. Barnett, Z. Keshavarz, A.G. Beer, D. Atwell, Acta Mater. 52 (2004) 5093.

[10] J. W. Christian, S. Mahajan, Prog. Mater. Sci. 39 (1995) 1 (espec. p.87).

[11] C. R. Heiple, S.H. Carpenter, J. Acoustic Emission 6 (1987) 177.

[12] J. Swiostek, J. Bohlen, D. Letzig, K. U. Kainer, Mat. Sci. Forum 488 – 489 (2005) 491.

[13] J. Swiostek, D. Letzig, K. U. Kainer, Proceedings of the First Russian International Conference and Exhibition of Magnesium – Broad Horizons, Nov 29th – Dec 01st 2005, accepted.

[14] K.B. Müller, in: H.I. Kaplan (ed.), Magnesium Technology 2002, TMS, 2002, 187.

[15] M. Bauser, G. Sauer, K. Siegert, Strangpressen (Textbook), Aluminium Verlag Düsseldorf, 2001.

[16] W.H. Sillekens, J.A.F.M. Schade van Westrum, A.J. den Bakker, P.-J. Vet, Materials Science Forum 426-432 - Proceedings of THERMEC’ 2003 – (2003) 629.

[17] V. Kree, J. Bohlen, D. Letzig, K.U. Kainer, Pract. Metallography 41 (2004) 233.

[18] Standard Practice for Acoustic Emission Examination of Fiberglass Reinforced Plastic Resin, ASTM E 1067-85. Tank/Vessels, May 31, 1985.

[19] E. Meza Garcia, P. Dobron, J. Bohlen, D. Letzig, F. Chmelik, K. U. Kainer, Mat. Sci. Eng. A (2006), this volume.

[20] J. Bohlen, F. Chmelik, P. Dobron, D. Letzig, P. Lukac, K. U. Kainer, J. Alloys Comp. 378 (2004) 214.

[21] C. H. J. Davies, S. Yi, J. Bohlen, K. U. Kainer, H.-G. Brokmeier, Mat. Sci. Forum 495 – 497 (2005) 1633.

[22] R. von Mises, Z. Angew. Math. Mech., 8 (1928) 161.

[23] G. Mann, J. R. Griffiths, C. H. Caceres, J. Alloys Comp. 378 (2004) 188.

[24] N. Ono, K. Nakamura, S. Miura, Mat. Sci. Forum 419 – 422 (2003) 195.

[25] P. Dobron, J. Bohlen, F. Chmelik, P. Lukac, D. Letzig, K. U. Kainer, Mat. Sci. Eng. A (2006) this volume.

[26] M.A. Gharghouri, G.C. Weatherly, J.D. Embury, Phil. Mag. A78 (1998) 1137.

Figure captions:

Fig. 1:

Tensile and compression yield strength as function of the inverse square root of the average grain size for extruded bars - solid squares: tensile yield strength, open circles: compressive yield strength, open triangles: lower compressive elastic limit, a) AZ31: $\sigma_{0\text{ tension}}$ = 147 (±2) MPa, $k_{y\text{ tension}}$ = 178 (±4) MPa·µm$^{1/2}$, $\sigma_{0\text{ compression}}$ = 45 (±5) MPa, $k_{y\text{ compression}}$ = 282 (±12) MPa·µm$^{1/2}$, b) AZ61: $\sigma_{0\text{ tension}}$ = 104 (±2) MPa, $k_{y\text{ tension}}$ = 251 (±5) MPa·µm$^{1/2}$, $\sigma_{0\text{ compression}}$ = 63 (±17) MPa, $k_{y\text{ compression}}$ = 292 (±38) MPa·µm$^{1/2}$, c) AZ80: $\sigma_{0\text{ tension}}$ = 120 (±2) MPa, $k_{y\text{ tension}}$ = 268 (±103) MPa·µm$^{1/2}$, $\sigma_{0\text{ compression}}$ = 81 (±33) MPa, $k_{y\text{ compression}}$ = 318 (±94) MPa·µm$^{1/2}$

Fig. 2:

Tensile/compression asymmetry as a function of inverse square root of the average grain size for extruded bars with a different content of aluminium (guidelines stem from related Hall - Petch data, see Figs. 1, and do not represent fits) - solid circles: AZ31, open squares: AZ61, open triangles: AZ80

Fig. 3:

Engineering stress strain curve (broken line) with AE count rates $\dot{N}_{C1}$ (solid line) and $\dot{N}_{C2}$ (dotted line) from a tensile test of an extruded bar, a) AZ31 (average grain size 16 µm), b) AZ61 (average grain size 12 µm), c) AZ80 (average grain size 12 µm)

Fig. 4:

Same as Fig. 3 but for compression tests, a) AZ31, b) AZ61, c) AZ80

Figures:

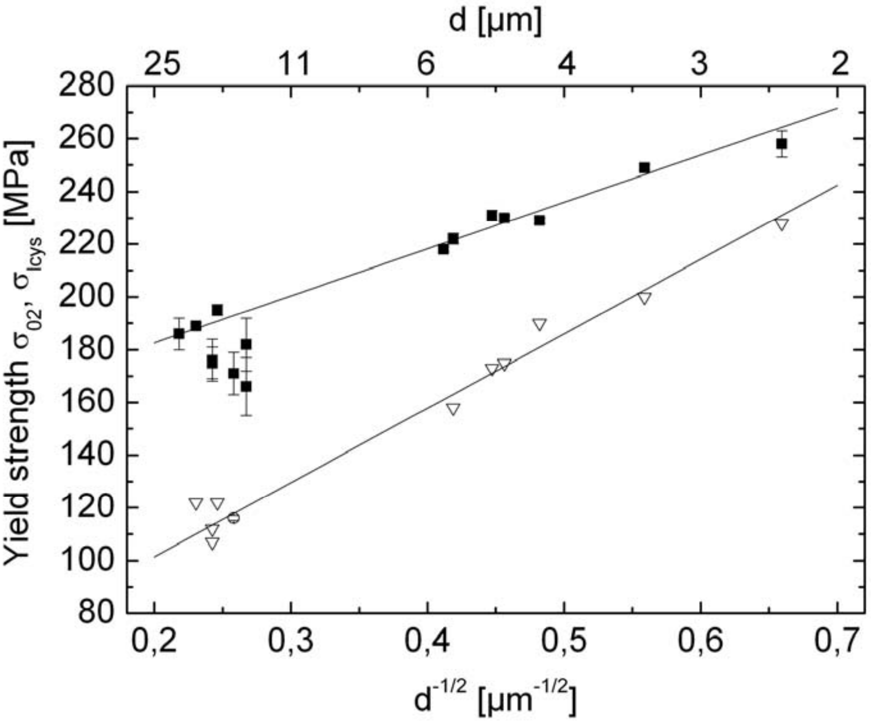

Fig. 1a

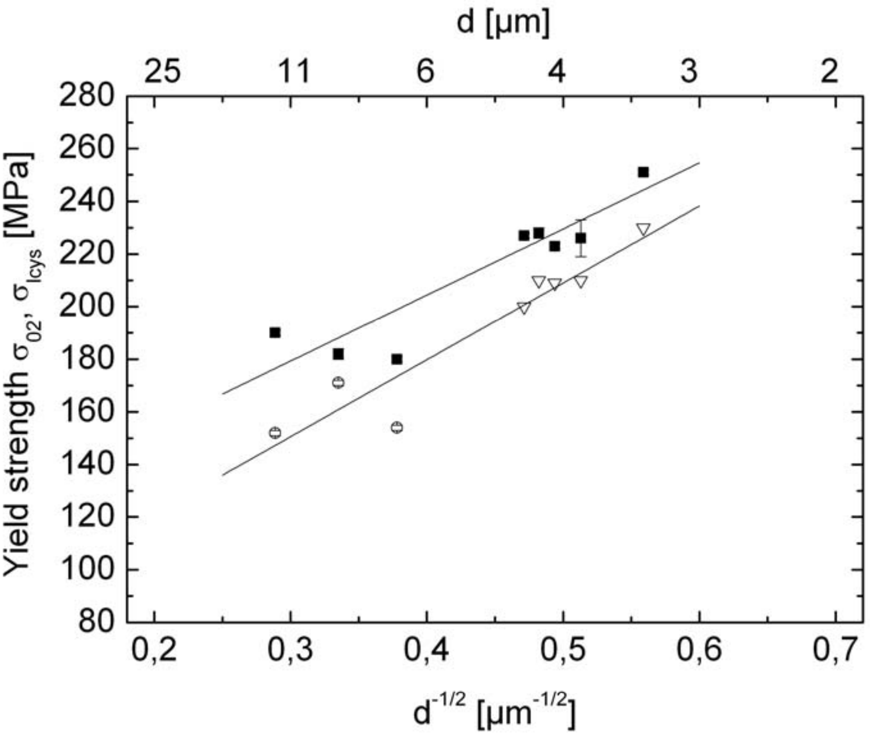

Fig. 1b

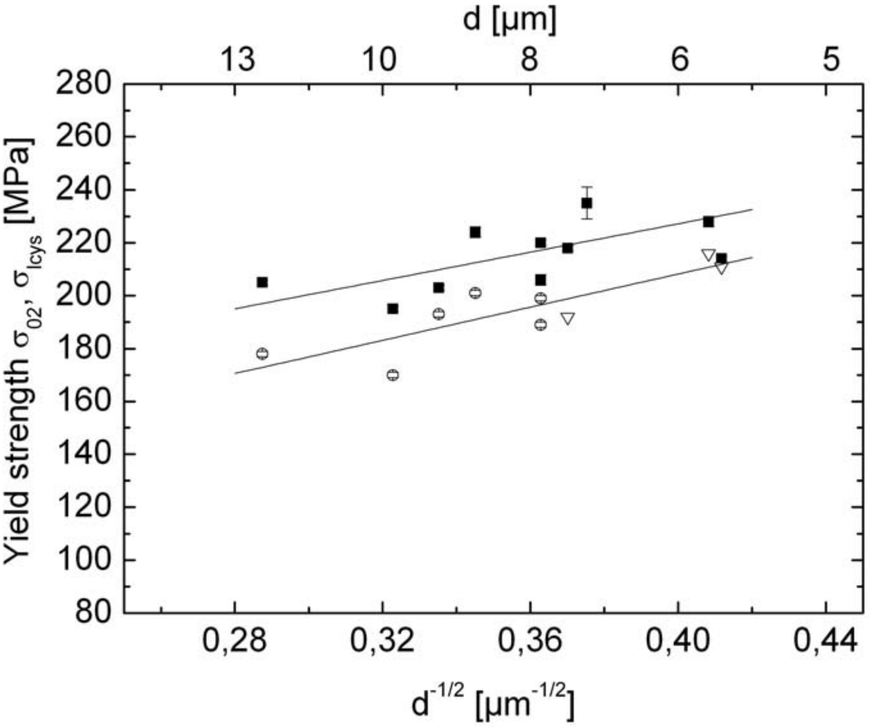
d [µm]
13
10
8
6
5
Yield strength σ_{02}, σ_{lcys} [MPa]
280
260
240
220
200
180
160
140
120
100
80
0,28
0,32
0,36
0,40
0,44
$d^{-1/2}$ [$\mu m^{-1/2}$]

Fig. 1c

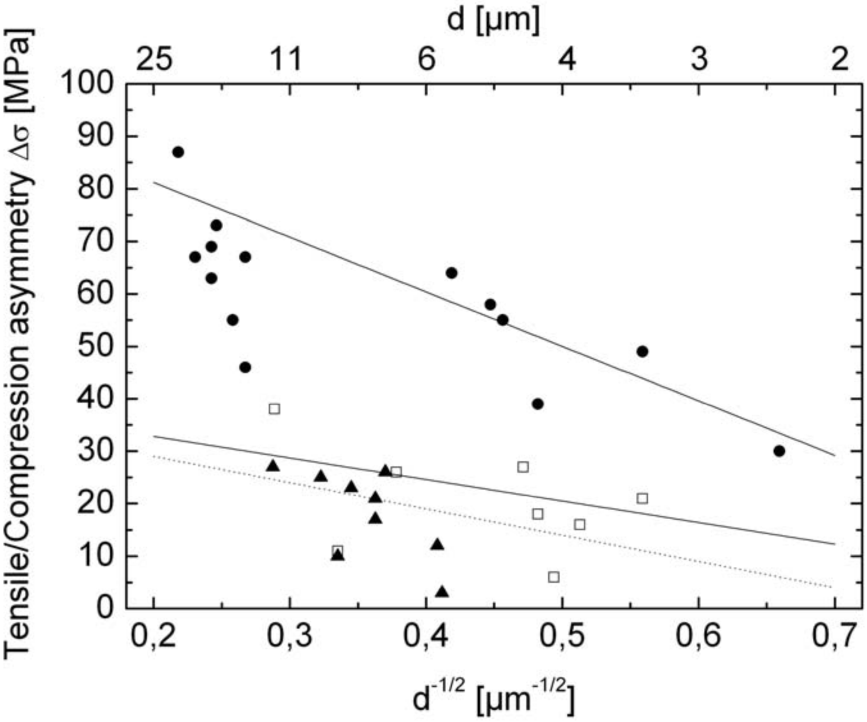
d [µm]
25
11
6
4
3
2
Tensile/Compression asymmetry $\Delta\sigma$ [MPa]
100
90
80
70
60
50
40
30
20
10
0
0,2
0,3
0,4
0,5
0,6
0,7
$d^{-1/2}$ [$\mu m^{-1/2}$]

Fig. 2

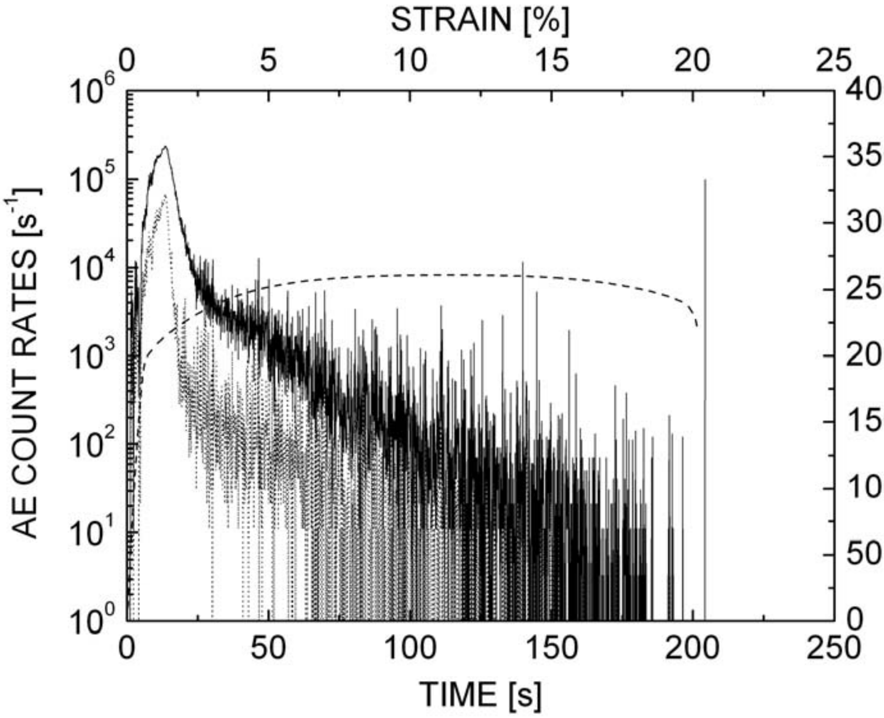
STRAIN [%]
0
5
10
15
20
25
10^6
10^5
10^4
10^3
10^2
10^1
10^0
AE COUNT RATES [s^{-1}]
400
350
300
250
200
150
100
50
0
STRESS [MPa]
0
50
100
150
200
250
TIME [s]

Fig. 3a

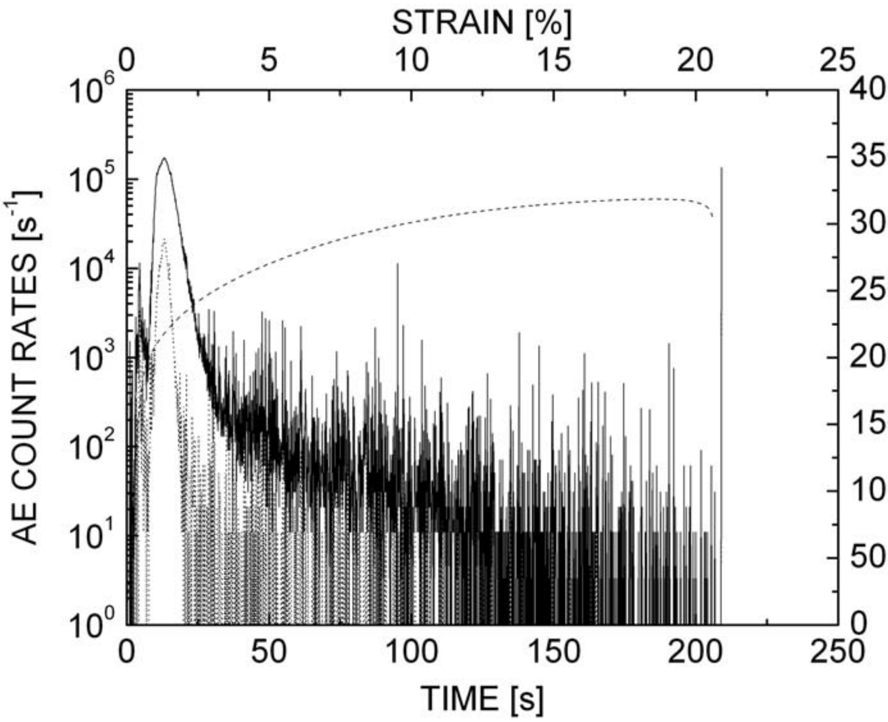
STRAIN [%]
0
5
10
15
20
25
10^6
10^5
10^4
10^3
10^2
10^1
10^0
AE COUNT RATES [s^{-1}]
400
350
300
250
200
150
100
50
0
STRESS [MPa]
0
50
100
150
200
250
TIME [s]

Fig. 3b

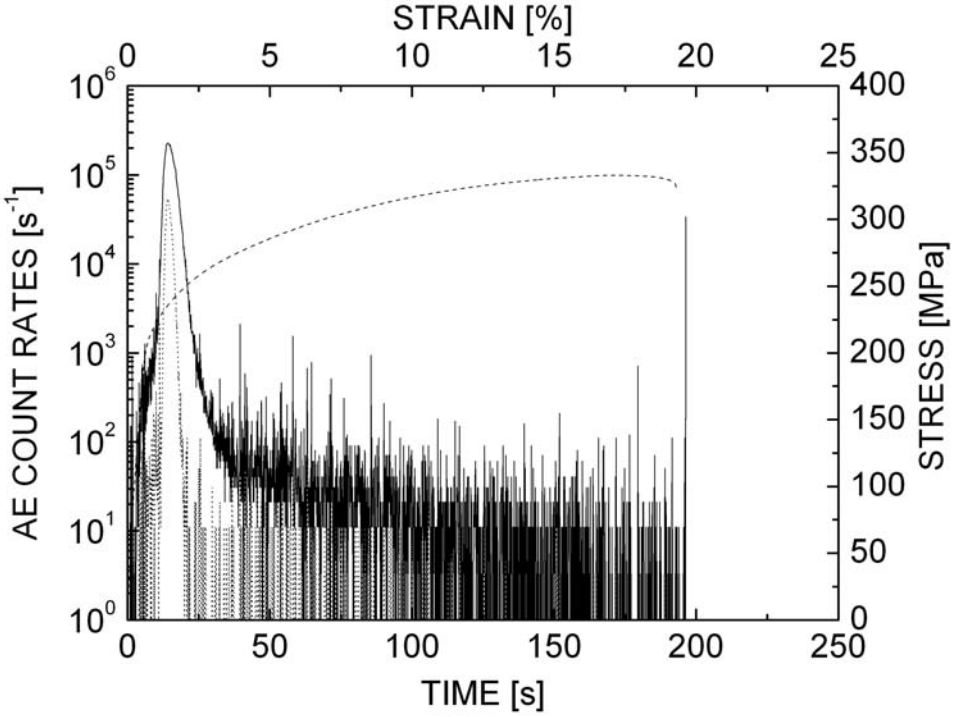
STRAIN [%]
0
5
10
15
20
25
AE COUNT RATES [s^{-1}]
10^0
10^1
10^2
10^3
10^4
10^5
10^6
STRESS [MPa]
0
50
100
150
200
250
300
350
400
TIME [s]
0
50
100
150
200
250

Fig. 3c

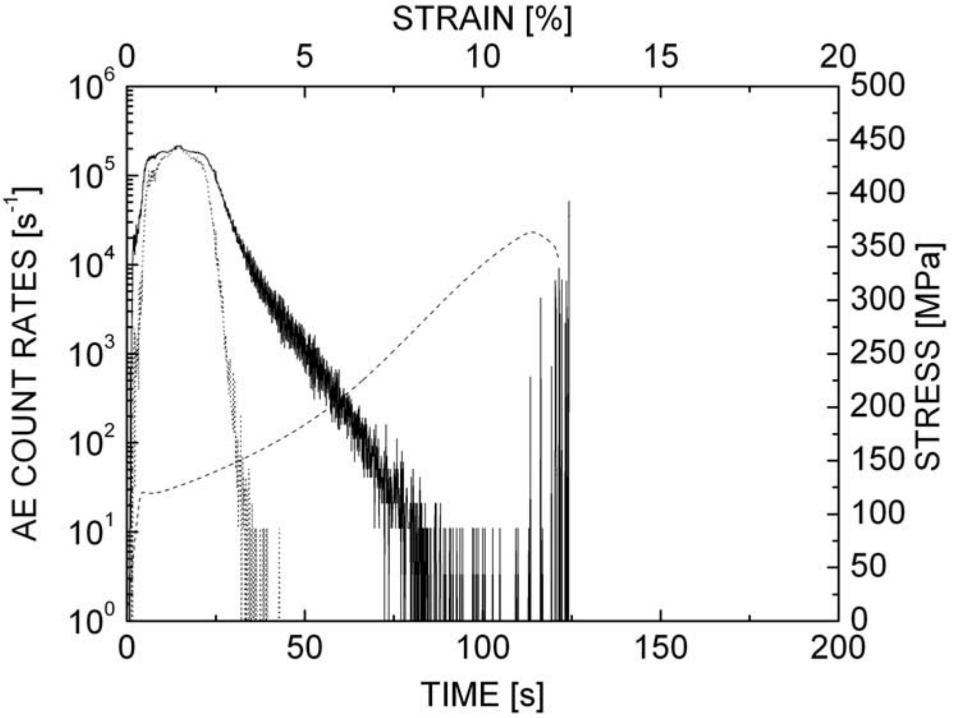
STRAIN [%]
0
5
10
15
20
AE COUNT RATES [s^{-1}]
10^0
10^1
10^2
10^3
10^4
10^5
10^6
STRESS [MPa]
0
50
100
150
200
250
300
350
400
450
500
TIME [s]
0
50
100
150
200

Fig. 4a

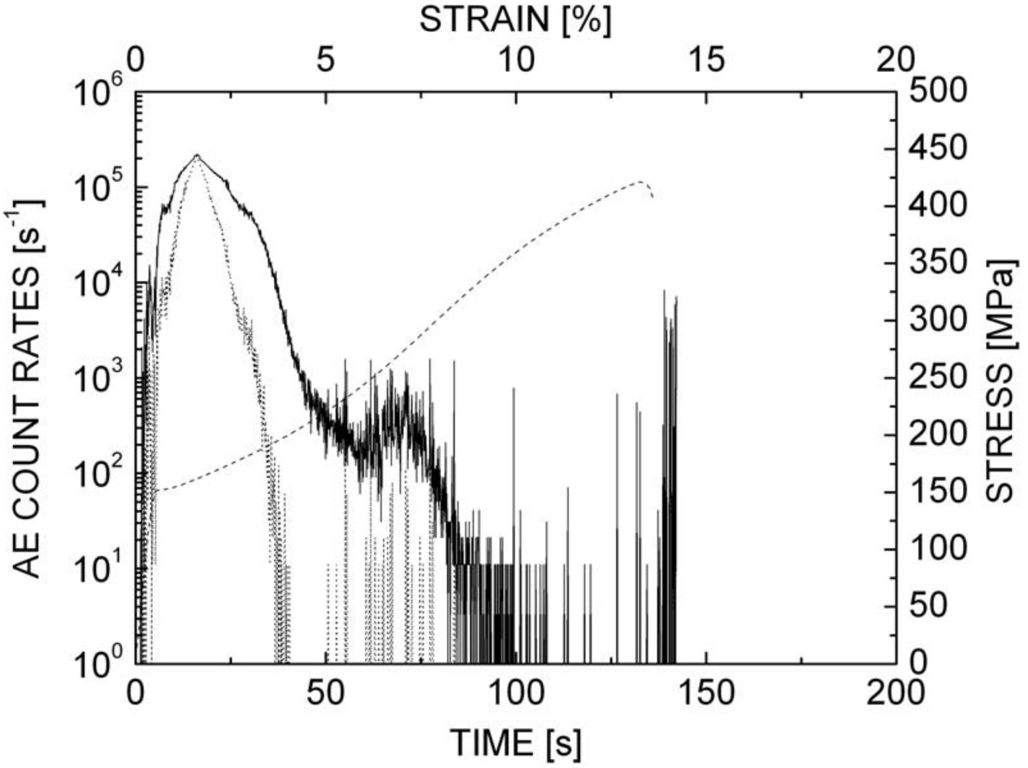
STRAIN [%]
0
5
10
15
20
10^6
10^5
10^4
10^3
10^2
10^1
10^0
AE COUNT RATES [s^{-1}]
500
450
400
350
300
250
200
150
100
50
0
STRESS [MPa]
0
50
100
150
200
TIME [s]

Fig. 4b

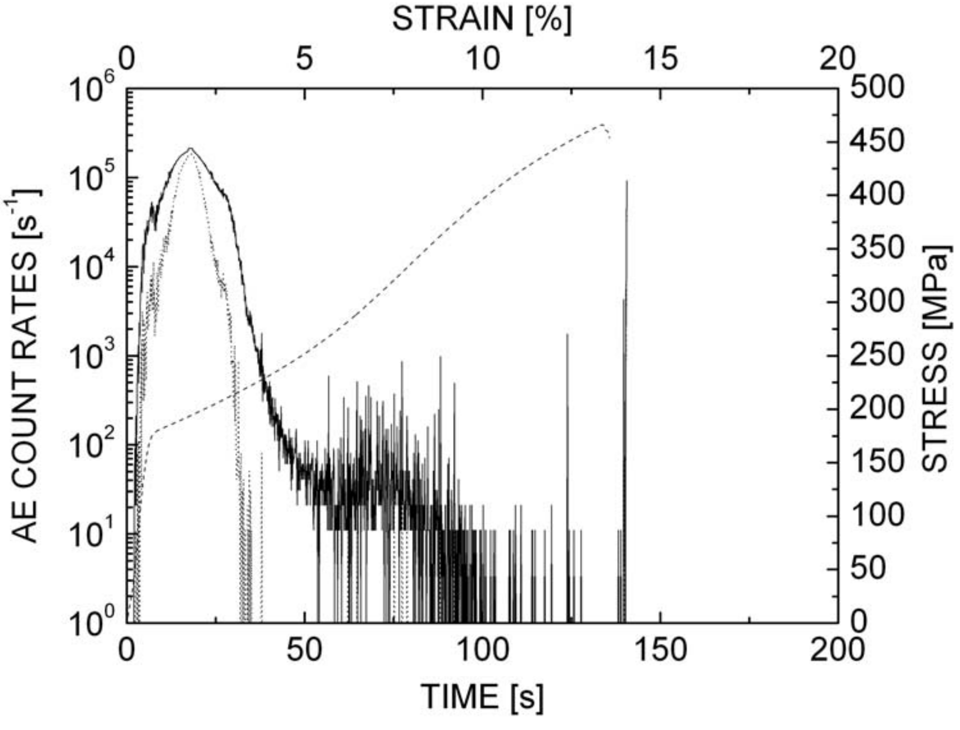
STRAIN [%]
0
5
10
15
20
10^6
10^5
10^4
10^3
10^2
10^1
10^0
AE COUNT RATES [s^{-1}]
500
450
400
350
300
250
200
150
100
50
0
STRESS [MPa]
0
50
100
150
200
TIME [s]

Fig. 4c